

Behaviour of the energy gap in a model of Josephson coupled Bose-Einstein condensates

A. P. Tonel^{1*}, J. Links¹ and A. Foerster²

¹ Centre for Mathematical Physics, School of Physical Sciences
The University of Queensland, Queensland, 4072, Australia

² Instituto de Física da UFRGS
Av. Bento Gonçalves 9500, Porto Alegre, RS - Brazil

July 7, 2018

Abstract

In this work we investigate the energy gap between the ground state and the first excited state in a model of two single-mode Bose-Einstein condensates coupled via Josephson tunneling. The energy gap is never zero when the tunneling interaction is non-zero. The gap exhibits no local minimum below a threshold coupling which separates a delocalised phase from a self-trapping phase that occurs in the absence of the external potential. Above this threshold point one minimum occurs close to the Josephson regime, and a set of minima and maxima appear in the Fock regime. Expressions for the position of these minima and maxima are obtained. The connection between these minima and maxima and the dynamics for the expectation value of the relative number of particles is analysed in detail. We find that the dynamics of the system changes as the coupling crosses these points.

PACS: 75.10.Jm, 71.10.Fd, 03.65.Fd

*sponsored by CNPq-Brazil

1 Introduction

Research into Bose-Einstein condensates (BECs) continues to attract considerable attention from both theoretical and experimental sides due to its contribution to the comprehension of physical phenomena emerging from mesoscopic systems. Recently, with the modernisation of experimental techniques, BECs have been produced and investigated by several research groups using magnetic traps with different kinds of confining geometries [1, 2] and chip devices [3, 4]. From the theoretical point of view, the model of two single-mode BECs coupled via Josephson tunneling (see eq. 1 in the next section and a comprehensive review in [5]) has been a successful model in further understanding the experimental realization of BECs in dilute alkali gases [6]. The success of this model is based on two main reasons: first is that despite its apparent simplicity, the model captures the physics behind the macroscopic quantum phenomena that emerge from these systems; second is that it is also applicable in other studies in mesoscopic solid state Josephson junctions [5, 7, 8], non-linear optics [9], statistical physics of spin systems [10, 11] and in nuclear physics [12, 13]. A theoretically important feature of this model is it can be formulated through the Quantum Inverse Scattering Method establishing solvability by Bethe Ansatz methods [14, 15].

Many aspects of this model have already been investigated, such as the dynamics of the population imbalance [16, 17, 19], the imbalance fluctuation [18, 19] and entanglement [9, 19–22] amongst others [23–25]. However an understanding of the properties of the energy gap as a function of the external potential, and an investigation of the dynamical consequences, appears lacking. This study is of interest since it could feasibly be tested in an experimental setting, particularly in cases where the external potential is the only tunable interaction, as may be expected in solid state systems. Here, we will expand on this aspect of the model by undertaking a detailed analysis of the energy gap behaviour across all coupling regimes. Specifically we will show that the energy gap function presents no local minimum below a threshold coupling, defined below, while above this threshold point one minimum occurs close to the Josephson regime and a set of minima and maxima appear in the Fock regime. The connection between these minima and maxima and the dynamics for the relative number of particles is investigated. We find that these minima and maxima act as a transition point separating entirely different dynamical behaviours.

The paper is organised in the following way. In section II we present the model and discuss the energy gap for different choices of the tunneling coupling and different regimes. In section III we discuss the correspondence between the minima and maxima that occur in the energy gap function and the temporal evolution for the relative number of particles in different regimes. In section IV we compare the quantum results with those obtained from a classical analysis. Section V is reserved for our conclusions.

2 Energy gap

The model we will study, based on the two-mode approximation as described in [5] (see also references therein), is described by the following Hamiltonian:

$$H = \frac{k}{8}(N_1 - N_2)^2 - \frac{\Delta\mu}{2}(N_1 - N_2) - \frac{\mathcal{E}_J}{2}(a_1^\dagger a_2 + a_2^\dagger a_1) \quad (1)$$

where a_i^\dagger, a_i ($i = 1, 2$) denote the single-particle creation and annihilation operators associated with two bosonic modes and $N_1 = a_1^\dagger a_1$ and $N_2 = a_2^\dagger a_2$ are the corresponding number operators. The quantity $N = N_1 + N_2$ is the total boson number operator and is conserved. The coupling k provides the strength of the interaction between the bosons, $\Delta\mu$ is the external potential and \mathcal{E}_J is the coupling for the tunneling. We mention that throughout we will take $k > 0$. The change $\mathcal{E}_J \rightarrow -\mathcal{E}_J$ corresponds to the unitary transformation $a_1 \rightarrow a_1, a_2 \rightarrow -a_2$, while $\Delta\mu \rightarrow -\Delta\mu$ corresponds to $a_1 \leftrightarrow a_2$. Therefore we will restrict our analysis to the case of $\mathcal{E}_J, \Delta\mu \geq 0$. It is useful to divide the parameter space into a number of regimes; viz. Rabi ($k/\mathcal{E}_J < 4/N$), Josephson ($4/N < k/\mathcal{E}_J \ll N$) and Fock ($k/\mathcal{E}_J \gg N$). In the Rabi and Josephson regimes, coherent superposition of the two condensates is expected whereas in the Fock regime the two condensates may be essentially localised. Note that we adopt the convention (cf. [26]) to specifically define the boundary between the Rabi and Josephson regimes by the threshold coupling $k/\mathcal{E}_J = 4/N$. This threshold was found in [16] as the transition coupling between macroscopic self-trapping ($k/\mathcal{E}_J > 4/N$) and delocalisation ($k/\mathcal{E}_J < 4/N$) for the case $\Delta\mu = 0$. (see also [19, 27, 28]). The presence of a non-zero external potential changes the coupling ratio at which this transition occurs, as we will show. However, it is useful to still refer to $k/\mathcal{E}_J = 4/N$ as the threshold coupling, irrespective of the value of the external potential, for other reasons which we will discuss.

Our main aim here is to investigate the behaviour of the energy gap for the Hamiltonian (1). In the Fock regime, we can preliminarily study this problem by putting the tunneling interaction term of the Hamiltonian (1) to zero, i.e. $\mathcal{E}_J = 0$. In this case all energy levels can be computed exactly. For the case of an even number of particles this yields

$$E_p = \frac{k}{2}p^2 + p\Delta\mu, \quad p = -\frac{N}{2}, -\frac{N}{2} + 1, \dots, -1, 0, 1, \dots, \frac{N}{2} - 1, \frac{N}{2}. \quad (2)$$

In the absence of the external potential ($\Delta\mu = 0$) the ground state is unique ($E_0 = 0$) and all other energies are double-degenerate, since $E_{-p} = E_p$. By switching on the external potential $\Delta\mu$, these degeneracies are broken.

Fixing the total boson number N and the interaction strength k and allowing the external potential $\Delta\mu$ to vary, expression (2) indicates two important facts: i) there are no degenerate energy levels, only level crossings; ii) all energies are functions of the value of the external potential value, except for $E_0 = 0$, and all energies of the type E_{-p} and E_0 correspond to the ground state in some region, defined by the strength of the external potential $\Delta\mu$. These regions are determined by the level crossings. Results are depicted in Fig. 1 for the case $N = 6, k = 6$.

The energy gap, in each region, is given by

$$\begin{aligned} \Delta_{(j+1,j)} &= E_{-j-1} - E_{-j} , & \Delta\mu \in [kj, k(j+1/2)] \\ \Delta_{(j-1,j)} &= E_{-j+1} - E_{-j} , & \Delta\mu \in [k(j-1/2), kj] \\ \Delta_{(N/2-1, N/2)} &= E_{-(N/2-1)} - E_{-N/2} , & \Delta\mu > k(N-1)/2. \end{aligned} \quad (3)$$

Here $\Delta_{(i,j)}$ ($\Delta_{(j,i)}$) denotes the energy gap before (after) the level crossing between the energy levels E_{-i} and E_{-j} . Notice that at each different region there is either a different ground state or a different first excitation. A similar structure has also been found in [29] by fixing all coupling parameters and varying the total number of particles.

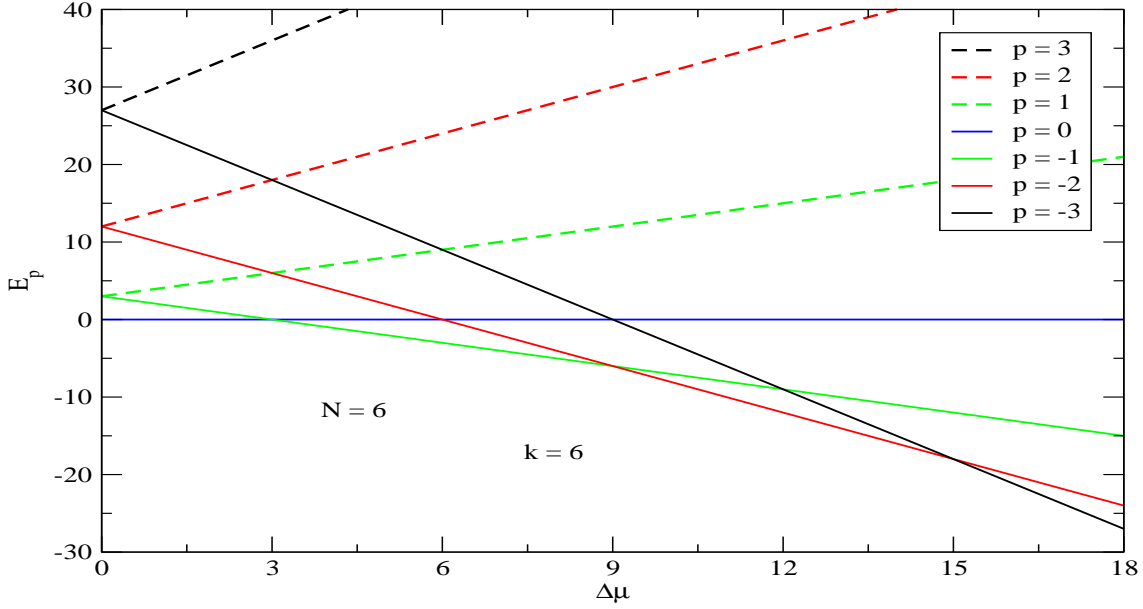


Figure 1: Energy levels versus the external potential for $N = 6$ and $k = 6$. The level crossings involving the lowest energy level represent changes in the ground state structure. The energy gap is also determined by level crossings involving the first excited state.

Considering the case of an odd total number of particles N , eq. (2) is still correct, however we have to eliminate the energy level E_0 and change the allowed values of the index p to $p = -N/2, -N/2 - 1, \dots, -1/2, 1/2, \dots, N/2 - 1, N/2$. Here, at $\Delta\mu = 0$, all energies are two-fold degenerate. By switching on the external potential $\Delta\mu$, all degeneracies are again broken and level crossings appear. Comparing the two cases, one can see that the gap behaviour of the model with external potential $\Delta\mu$ and an odd number of particles N is the same as the profile for a system with $N + 1$ particles and external potential $\Delta\mu + k/2$.

Now we consider the situation where the coupling \mathcal{E}_J between the two condensates is switched on and we study its effect using the numerical diagonalisation of the Hamiltonian (1). In terms of the energy gap, the existence of the threshold coupling is suggested by the curve of the energy gap as a function of the external potential. Above the threshold ($k/\mathcal{E}_J > 4/N$), one or more local minima appear while no local minimum occurs when $k/\mathcal{E}_J < 4/N$. Let us first focus our attention on the analysis of the energy gap in the region above the threshold point, in particular, in the region where $k/\mathcal{E}_J \geq 1$. In Fig. 2 we plot the energy gap Δ versus the external potential $\Delta\mu$ with different values of the coupling parameter \mathcal{E}_J for the cases $N = 6, 7$.

We can see clearly the effect produced by the tunneling term \mathcal{E}_J . Before switching on this coupling, in the extreme Fock regime ($\mathcal{E}_J = 0$), the energy gap curve is not differentiable at each minima and maxima. Here the maxima and minima are determined by level crossing and, consequently, either a change in the ground state or the first excited state.

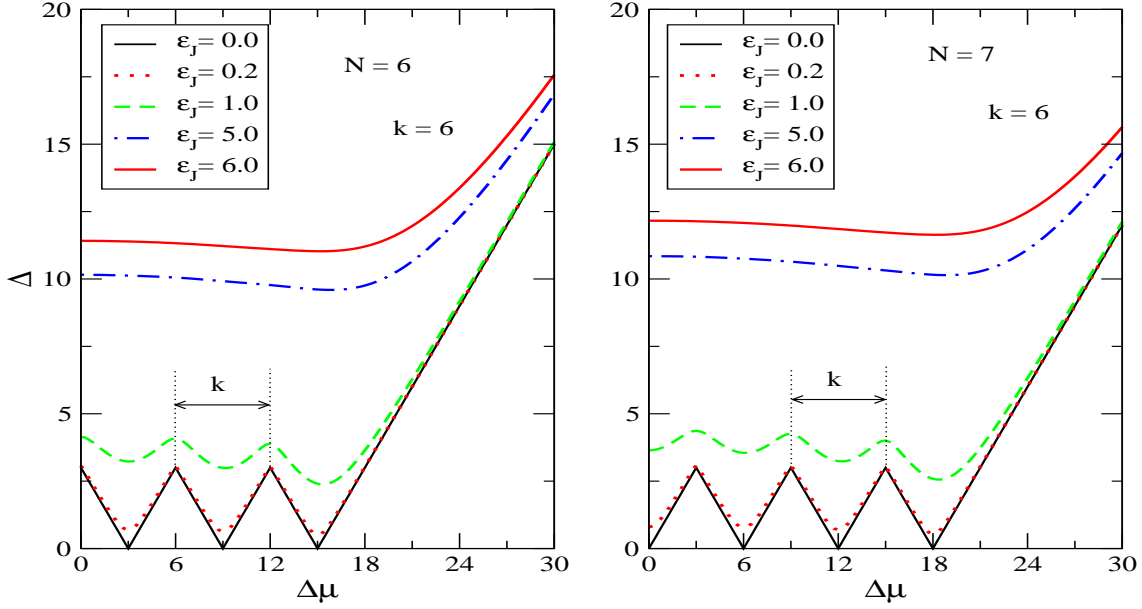


Figure 2: Energy gap Δ versus the external potential $\Delta\mu$ for different choices of the coupling parameter $\mathcal{E}_J = 0, 0.2, 1, 5, 6$. On the left, $N = 6$, and on the right, $N = 7$. In the extreme Fock regime ($\mathcal{E}_J = 0$) the minima and maxima represent the level crossings as depicted in Fig. 1. For small values of \mathcal{E}_J the difference between two consecutive minima or maxima is constant and equal to k . As \mathcal{E}_J increases just one minimum survives.

In this particular situation we can exactly calculate the energy gap value in all regions using equations (2, 3). It is interesting to observe that at each minimum (respectively maximum) the same value for the energy gap is found.

Turning on the coupling term \mathcal{E}_J the energy gap function becomes smooth. An important fact here is that weak tunneling does not considerably change the position of the minima and maxima in relation to the $\mathcal{E}_J = 0$ case. It does change, however, the value of the energy gap at each minimum and maximum. This effect is strongest in the first region ($\Delta\mu \in [0, k/2]$), reducing gradually at each subsequent region, with the last minimum corresponding to the lowest value of the gap. Increasing the value of the coupling term \mathcal{E}_J to take the model out of the Fock regime leads to a suppression in the number of minima and maxima until just one minimum survives.

We now look closer at the set of minima and maxima that appear in the Fock regime. The number of these minima and maxima depends on the total number of particles N . If N is even, the number of maxima and minima is the same, $N/2$, while if N is odd the number of minima is $(N + 1)/2$ and the number of maxima is $(N - 1)/2$. However, we find that the difference between two consecutive minima (or maxima) is always constant and equal to k independent of the total number of particles. This allows us to examine a general expression for the position of each minimum and maximum of the energy gap that occurs with respect to the external potential, which we find fits very well with

$$\Delta\mu_c = \frac{N-l}{2}k + \frac{\mathcal{E}_J}{N^2}, \quad l = 1, 2, 3, \dots, N. \quad (4)$$

Above, odd choices for the index l ($l = 1, 3, 5, 7, \dots$) generate the minima, while even choices ($l = 2, 4, 6, 8, \dots$) the maxima. The particular choice $l = 1$ corresponds to the lowest minimum, while $l = 3$ the second lowest minimum, and so on. With the exception of the lowest minimum, all other minima and maxima disappear as the ratio \mathcal{E}_J increases. This is illustrated in Fig. 2, for $\mathcal{E}_J = 5, 6$ corresponding to the situation where we approach the Josephson regime after leaving the Fock regime. For $k/\mathcal{E}_J \geq 1$ (Josephson and Fock regimes), we find that the position of the minimum can still be determined by the previous expression (4) using $l = 1$.

In the interval $k/\mathcal{E}_J \in (4/N, 1]$ the energy gap function still has a local minimum, however the position at which this occurs is not longer given by (4) and we have not been able to find a simple expression for it. The value of $\Delta\mu$ at which the minimum occurs approaches zero as the ratio k/\mathcal{E}_J approaches the threshold coupling. Further decreasing the ratio k/\mathcal{E}_J past the threshold point toward the Rabi regime, we find a new scenario: the energy gap is now a monotonic function for all values of $\Delta\mu$. This behaviour is illustrated in Fig. 3, where we plot the energy gap function versus the external potential $\Delta\mu$ in the region $k/\mathcal{E}_J \leq 1$ (Josephson and Rabi regimes, including the threshold point) for $N = 40$ particles. In these cases differences between even and odd particle numbers are not significant as the strength of the tunneling term dominates any parity effects due the external potential.

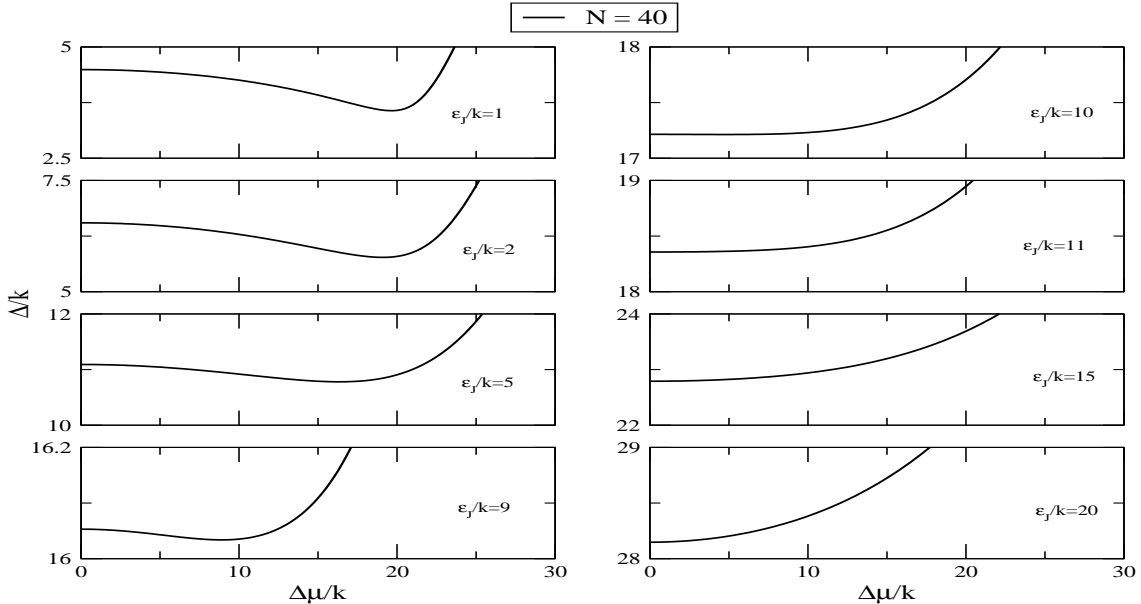


Figure 3: Energy gap versus the external potential for $N = 40$ and different choices of the parameter ratio $\mathcal{E}_J/k = 1, 2, 5, 9, 10, 11, 15, 20$. On the left (right) side we display the points below (above) the threshold point $\mathcal{E}_J/k = 10$. On the left hand side we can clearly see the existence of a minimal energy gap, while on the right hand side the energy gap is a monotonic function of the external potential.

We emphasise that (4) was obtained by numerical fitting. It is useful to see how this result compares with the predictions of perturbation theory. It was argued in [14] that for the weak tunneling regime perturbation results are only valid for the Fock regime $\mathcal{E}_J \ll k/N$. A standard calculation using degenerate perturbation theory shows that to first order there is no correction to the values of the applied potential which give the minimal energy gaps; i.e.

$$\Delta\mu_{\text{pert}} = \frac{N-l}{2}k, \quad l = 1, 3, 5, 7, \dots$$

To make comparison between (4) and this perturbative result we note that for the Fock regime

$$\begin{aligned} \frac{N-l}{2}k &< \Delta\mu_c \\ &= \frac{N-l}{2}k + \frac{\mathcal{E}_J}{N^2} \\ &< \frac{N-l}{2}k + \frac{k}{N^3} \\ &= \left(\frac{N-l}{2} + \frac{1}{N^3} \right) k, \end{aligned}$$

i.e.

$$\frac{N-l}{2}k < \Delta\mu_c < \left(\frac{N-l}{2} + \frac{1}{N^3} \right) k.$$

Thus the formula (4) agrees with the perturbative result up to a small correction of order N^{-3} . It is important to stress however our numerical result (4) applies also in the Josephson regime where the perturbative result is not valid.

It was also argued in [14] that perturbation results for strong tunneling are only valid for $\mathcal{E}_J \gg kN$. Our numerical results show that the existence of minima for the gap only occurs for couplings $\mathcal{E}_J < kN/4$, which does not intersect the perturbative strong tunneling regime.

In the next section, we will discuss the influence of the gap on the quantum dynamics for the relative number of particles. In particular, we will show that the choice of couplings corresponding to the minimal and maximal points of the energy gap represent transition points separating different types of dynamical behaviour. Fortunately, we can identify all these points using eq. (4) above.

3 Quantum dynamics

We will investigate the quantum dynamics using the same methods we employed in [19]. The time evolution of any state is determined by $|\Psi(t)\rangle = U(t)|\phi_0\rangle$, where U is the temporal evolution operator given by $U(t) = \sum_{m=0}^M |m\rangle\langle m| \exp(-iE_m t)$, $|m\rangle$ is an eigenstate with energy E_m and $|\phi_0\rangle$ represents the initial state. Using these expressions we can compute the expectation value of the relative number of particles

$$\langle(N_1 - N_2)(t)\rangle = \langle\Psi(t)|N_1 - N_2|\Psi(t)\rangle. \quad (5)$$

In Fig. 4 we plot the expectation value for the relative number of particles in the Josephson regime ($k/\mathcal{E}_J = 1$) for different ratios of the coupling $\Delta\mu/\mathcal{E}_J$ for $N = 50, 100$ and with the initial state $|N, 0\rangle$.

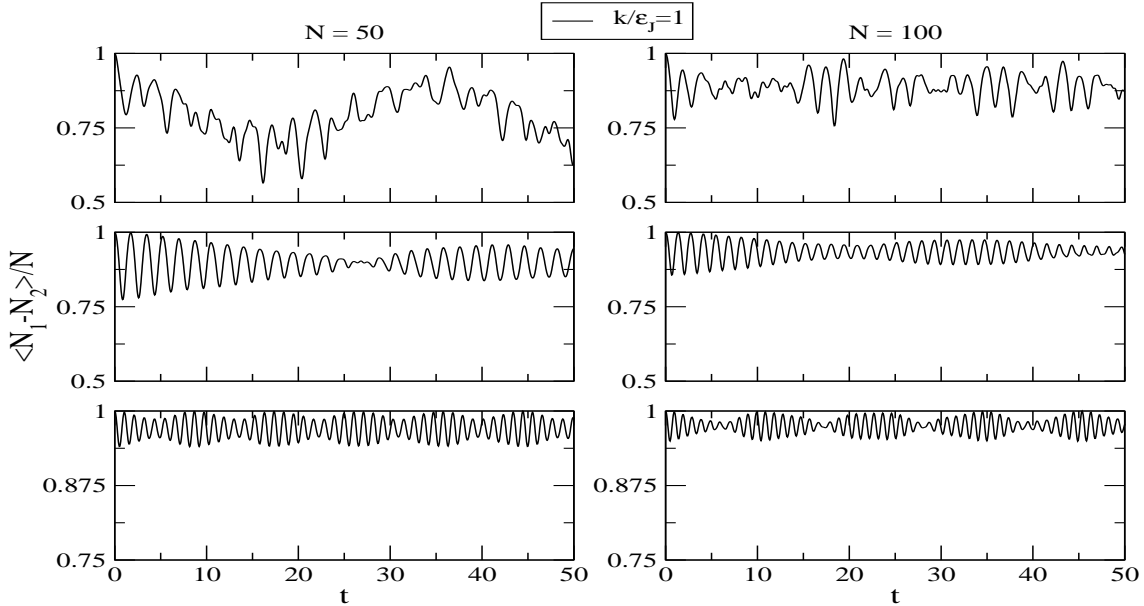


Figure 4: Time evolution of the expectation value of the relative number of particles in the Josephson regime $k/\mathcal{E}_J = 1$ ($\mathcal{E}_J = 1$), for $N = 50, 100$. The initial state is $|N, 0\rangle$. The central graph corresponds to the configuration where the energy gap is a minimum, at $\Delta\mu_c/\mathcal{E}_J = 24.5, 49.5$. The other graphs represent points before and after this minimum point given by $\Delta\mu/\mathcal{E}_J = \Delta\mu_c/\mathcal{E}_J \mp 5$.

The central graph in each column represents the dynamics when the system is in the configuration where the energy gap is minimal, which can be calculated through eq. (4). This corresponds to $\Delta\mu_c/\mathcal{E}_J = 24.5, 49.5$ for the cases $N = 50, 100$, respectively. The other graphs in each column, above and below, depict the dynamics for cases where $\Delta\mu/\mathcal{E}_J = \Delta\mu_c/\mathcal{E}_J \mp 5$ in Fig. 4. The coupling corresponding to the minimal energy gap signifies a point where the dynamics changes drastically: before it the behaviour is clearly non-periodic (the first box in each column), while after it the oscillations follow a collapse and revival sequence (the last box in each column). A noticeable feature here is that in the same region, both graphs $N = 50, 100$ show basically the same qualitative behaviour. The collapse and revival pattern, however, is more pronounced when the number of particles is larger. Further increasing the ratio $\Delta\mu/\mathcal{E}_J$ beyond the value corresponding to the minimal energy gap, the behaviour is still of a collapse and revival type, however the amplitude of oscillation and the collapse and revival time both decrease.

Next we turn our attention to study the connection between the dynamics and the energy gap for the crossover region between the Josephson and Fock regimes, where a set

of minima and maxima in the energy gap appear as a function of the external potential. Again, the position of these minima and maxima can be obtained from eq. (4). In Fig. 5 we plot the temporal evolution of the expectation value for the relative number of particles for the case $N = 50$ for the coupling ratio $k/\mathcal{E}_J = 60$, using the initial state $|N, 0\rangle$. The central graph in each column represents the point where the energy gap is minimal ($l = 1, 3$) or maximal ($l = 2, 4$), occurring at $\Delta\mu_c/\mathcal{E}_J = 1470, 1440, 1410, 1380$ (from left to right). The other graphs above (respectively below) in each column represent the dynamics for the situation where $\Delta\mu$ is smaller (respectively larger) than $\Delta\mu_c$. The first and third columns represent the dynamics for cases where the energy gap is near the two lowest minima, while the second and fourth represent the behavior near the two lowest maxima.

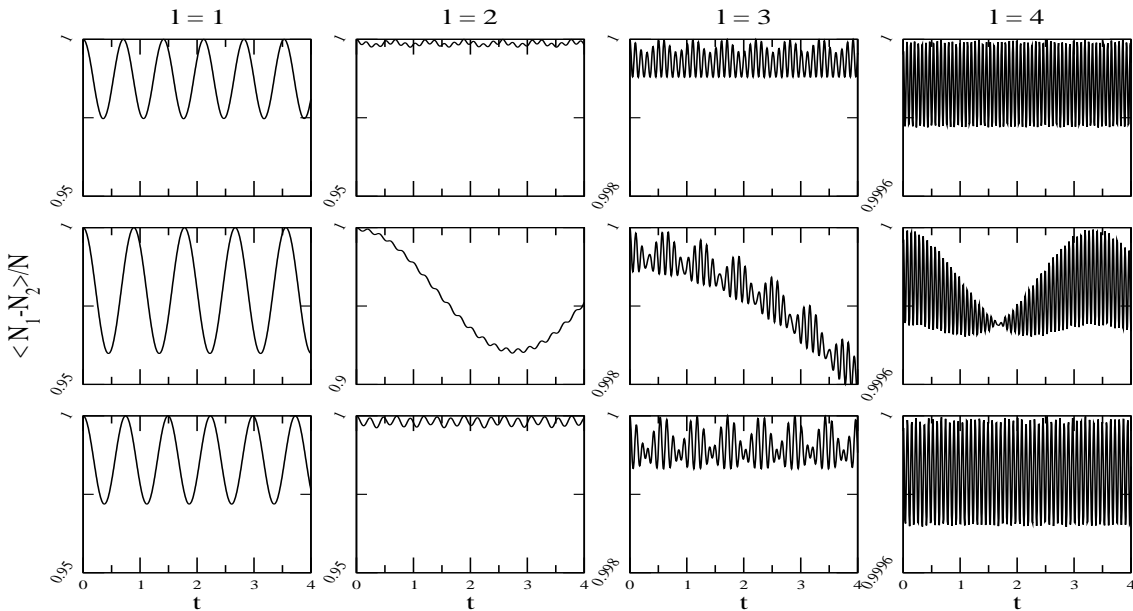


Figure 5: Dynamics of the expectation value of the relative number of particles for $N = 50$, $k/\mathcal{E}_J = 60$ ($\mathcal{E}_J = 1$) and with the initial state $|N, 0\rangle$. The central graph, at each column, represents the point where the energy gap is minimal ($l = 1, 3$) or maximal ($l = 2, 4$), occurring at $\Delta\mu_c/\mathcal{E}_J = 1470, 1440, 1410, 1380$ (from left to right). In each case the graphs above and below show dynamics of points around the minimum or maximum, chosen as $\Delta\mu/\mathcal{E}_J = \Delta\mu_c/\mathcal{E}_J \mp 5$. It is clear that each minimum and maximum signifies a change in the dynamical behaviour.

The minima and maxima for the energy gaps represent frontiers between different types of oscillations in the neighbourhood of these points. After the last minimum at $l = 1$ the expectation value evolves periodically, as in the last graph of the first column. However, the amplitude of the oscillations becomes smaller as the ratio $\Delta\mu/\mathcal{E}_J$ becomes larger.

Finally we investigate the dynamics for the situation where the system is below the threshold coupling ($k/\mathcal{E}_J < 4/N$) where the energy gap does not exhibit a local minimum, as already mentioned. In Fig. 6 we plot the expectation value for the relative number of particles for different choices of the ratio \mathcal{E}_J/k in the regime between Josephson and Rabi for $N = 40$ and using the initial state $|N, 0\rangle$. Here the dynamics displays collapse and revival of oscillations for any value of the external potential. The presence of an external potential increases the collapse and revival time, which tends to infinity as the external potential approaches infinity. Moreover, increasing the external potential also leads the system out of a delocalised phase into one of self-trapping. In fact, it is apparent that for any choice of \mathcal{E}_J/k one can choose a suitably large $\Delta\mu$ which will dominate the dynamics and the system will necessarily display self-trapping.

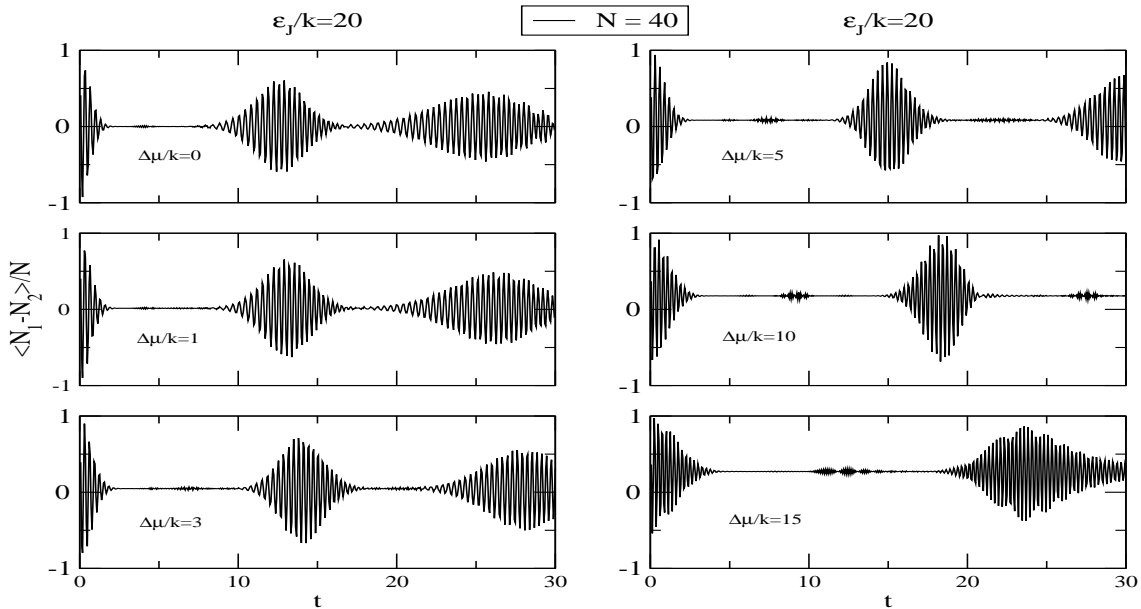


Figure 6: Expectation value for the relative number of particles versus time for different values of the external potential in the regime between Josephson and Rabi (below the threshold coupling). Here,, we are fixing $\mathcal{E}_J = 20$ and $k = 1$ The initial state is $|N, 0\rangle$ with $N = 40$. Increasing the external potential produces increasing collapse and revival time and also leads to a self-trapping phase.

4 Classical dynamics

Here we compare the above results with those that are obtained by an analogous classical analysis of the model. Defining $z = (N_1 - N_2)/N$ we may equivalently consider the

Hamiltonian [26, 30]

$$H(z, \phi) = \frac{\mathcal{E}_J N}{2} \left(\frac{\lambda}{2} z^2 - \beta z - \sqrt{1 - z^2} \cos(2\phi/N) \right) \quad (6)$$

where

$$\lambda = \frac{kN}{2\mathcal{E}_J}, \quad \beta = \frac{\Delta\mu}{\mathcal{E}_J}$$

and z, ϕ are canonically conjugate variables. The Hamiltonian (6) obeys the symmetries

$$\begin{aligned} H(z, \phi)|_{\lambda, \beta} &= -H(z, \phi + N\pi/2)|_{-\lambda, -\beta} \\ H(z, \phi)|_{\lambda, \beta} &= H(-z, \phi)|_{\lambda, -\beta}. \end{aligned}$$

In the usual way the dynamics is given by Hamilton's equations

$$\dot{\phi} = \frac{\partial H}{\partial z} = \frac{\mathcal{E}_J N}{2} \left(\lambda z - \beta + \frac{z}{\sqrt{1 - z^2}} \cos(2\phi/N) \right) \quad (7)$$

$$\dot{z} = -\frac{\partial H}{\partial \phi} = -\mathcal{E}_J \left(\sqrt{1 - z^2} \sin(2\phi/N) \right). \quad (8)$$

The classical dynamical evolution of the system is constrained to the level curves of H in phase space. The nature of the level curves is largely determined by the fixed points of H determined by $\dot{z} = \dot{\phi} = 0$, and transitions in the dynamical behaviour can be identified with fixed point bifurcations. We find the following classification of the fixed points:

- $\phi = 0$ and z is a solution of

$$\lambda z = -\frac{z}{\sqrt{1 - z^2}} + \beta \quad (9)$$

which has a unique real solution for $\lambda \geq 0$. For this solution the Hamiltonian attains a local minimum.

- $\phi = N\pi/2$ and z is a solution of

$$\lambda z = \frac{z}{\sqrt{1 - z^2}} + \beta. \quad (10)$$

This equation has either one or three real solutions.

a) $0 \leq \lambda < 1$

For any value of β there is just one real solution, for which the Hamiltonian attains a local maximum.

b) $\lambda > 1$

Here a transition value for β_c appears, which is dependent on λ . For $\beta < \beta_c$, the equation has two locally maximal solutions and one saddle point, while for $\beta > \beta_c$ the equation has just one real solution, a locally maximal fixed point. Thus a fixed point bifurcation occurs at β_c .

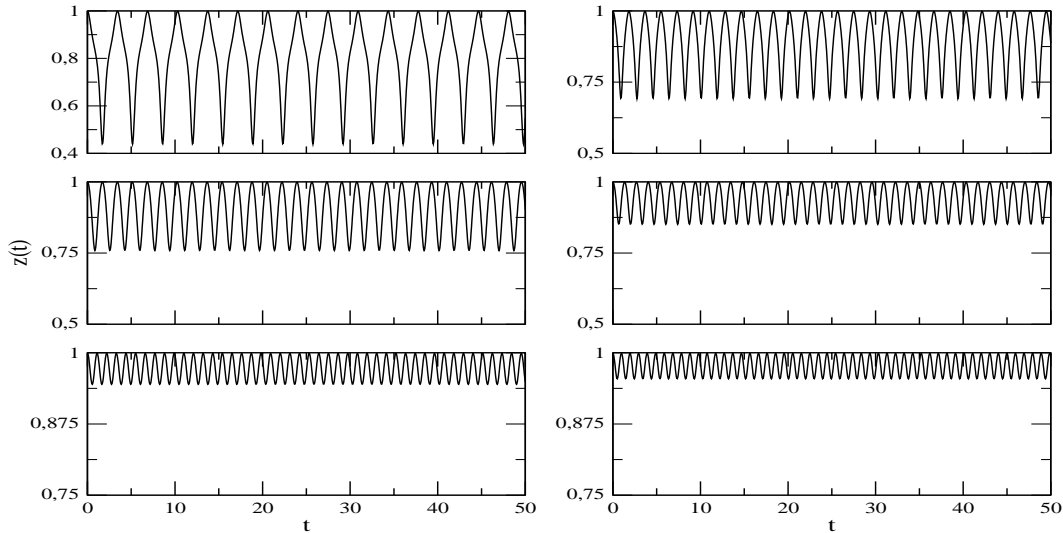


Figure 7: Classical time evolution of the relative number of particles in the Josephson regime $k/\mathcal{E}_J = 1$, for $N = 50, 100$. The initial condition is $z \simeq 1$, $\phi = 0$. The central graph corresponds to the configuration where for the quantum model the energy gap is a minimum, at $\Delta\mu_c/\mathcal{E}_J = 24.5, 49.5$. The other graphs represent points before and after this minimum point given by $\Delta\mu/\mathcal{E}_J = \Delta\mu_c/\mathcal{E}_J \mp 5$.

We remark that in the case $\lambda = 1$ the transition value is given by $\beta_c = 0$. Thus in the absence of the external potential the classical dynamics predicts a transition coupling of $k/\mathcal{E}_J = 2/N$ [26], whereas for the quantum dynamics the threshold between delocalisation and self-trapping occurs at $k/\mathcal{E}_J = 4/N$ [16, 19]. The difference between the classical and quantum cases may be explained in terms of the uncertainty relation between z and ϕ .

It is apparent that the analysis of the classical system for non-zero external potential only predicts one transition point, which can be identified as a fixed point bifurcation. In contrast we have shown above that for the quantum dynamics there are several points associated with minima and maxima of the energy gap, for which there is a qualitative transition in the dynamical behaviour. In Figs. (7,8,9) below, we show the dynamical behaviour predicted by the classical Hamiltonian using the same initial conditions and coupling parameters for the cases shown in Figs. (4,5,6) respectively. In particular, in figure 9 we present both, the classical and the quantum curves in a shorter time interval for a better comparison.

In most cases the results predicted by the quantum and classical analyses agree for sufficiently small time intervals, a feature also observed in [16]. In all cases however, there are stark differences in the dynamics over long time intervals. The irregular behaviour appearing below the transition coupling in Fig. 4 does not occur in Fig. 7. The dynamical transitions that are shown in the last three columns of Fig. 5 are not apparent from the classical results of Fig. 8. And the collapse and revival of oscillations which is clear in the quantum dynamics (Fig.6 and the solid curve in Fig.9) is not seen in the classical case given by the dashed curve in Fig. 9.

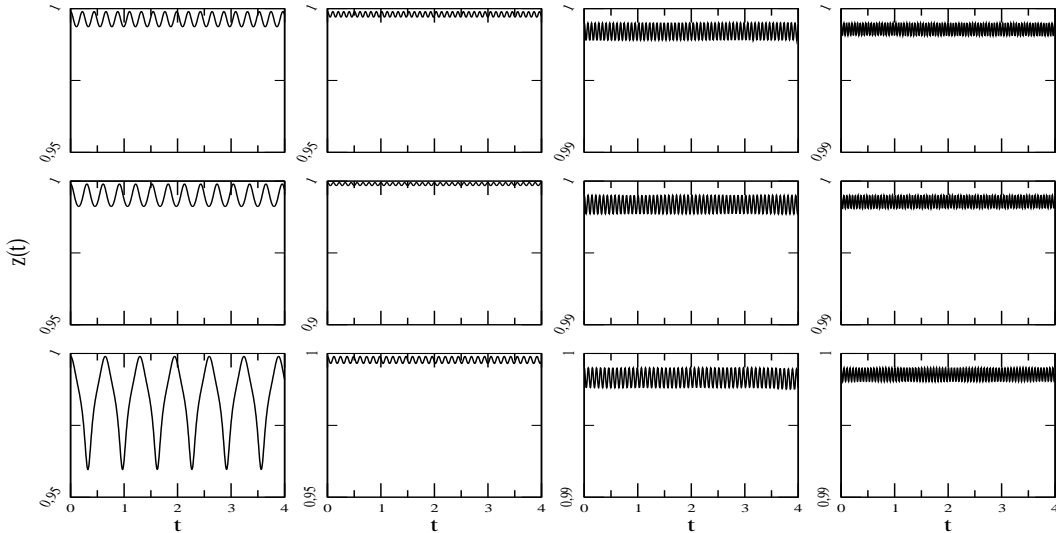


Figure 8: Classical dynamics of the relative number of particles for $N = 50$, $k/\mathcal{E}_J = 60$ and with the initial condition $z \simeq 1$, $\phi = 0$. The central graph, at each column, represents the point where for the quantum model the energy gap is minimal ($l = 1, 3$) or maximal ($l = 2, 4$), occurring at $\Delta\mu_c/\mathcal{E}_J = 1470, 1440, 1410, 1380$ (from left to right). In each case the graphs above and below show dynamics of points around the minimum or maximum, chosen as $\Delta\mu/\mathcal{E}_J = \Delta\mu_c/\mathcal{E}_J \mp 5$.

5 Summary

To summarise, we have studied the nature of the energy gap as a function of the external potential and its connection to the dynamical behaviour. We have shown that the energy gap function presents no minimum below the threshold coupling, while above this threshold point one minimum occurs close to the Josephson regime and a set of minima and maxima appear in the Fock regime. We found that the total number of these minima and maxima depends only on the number of particles. An explicit expression for the position of these minima and maxima was given. The connection between these energy gap extrema and the dynamics for the relative number of particles was investigated, and it was found that the extrema determine transition points separating different dynamical behaviours. We have also compared these results with those that are obtained from a classical analysis of the Hamiltonian.

Finally, we refer to recent experimental work [31] where both delocalisation, with tunneling times of the order 50 ms, and self-trapping have been confirmed in a single bosonic Josephson junction with a symmetric double-well potential using a Bose-Einstein condensate of ^{87}Rb atoms. In this experimental setup both scenarios were observed by simply varying the total atomic population N . We note that from equation (4) it can be seen that for fixed coupling parameters k , $\Delta\mu$ and \mathcal{E}_J , the transition couplings $\Delta\mu_c$ can be tuned by also varying the total population N . Thus the results we have obtained above are relevant for the experimental system of [31] with an asymmetric potential.

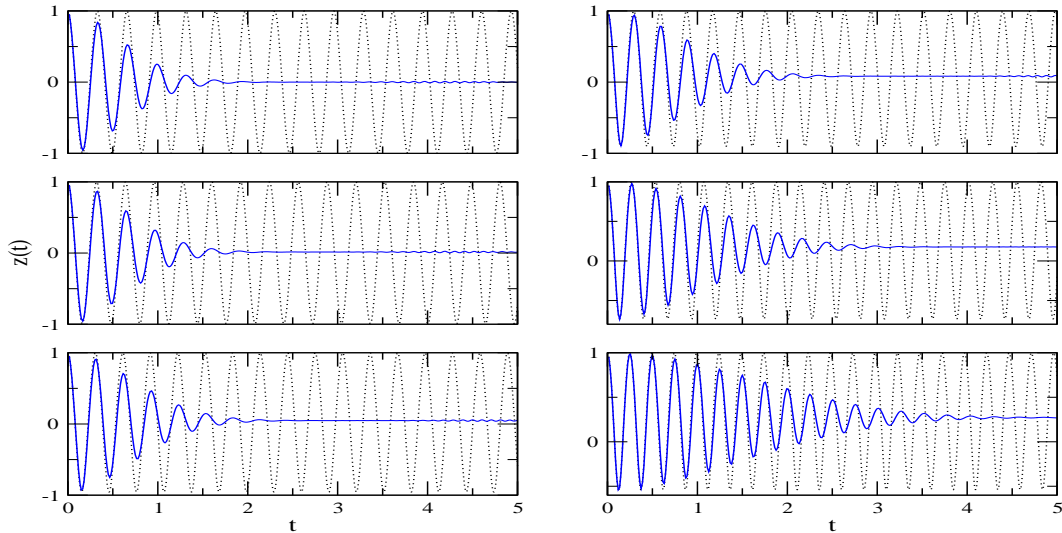


Figure 9: Classical (dashed line) and quantum (solid line) evolution of the relative number of particles versus time for different values of the external potential (from the top to the bottom: $\Delta\mu/k = 0, 1, 3$ on the left and $\Delta\mu/k = 5, 10, 15$ on the right) in the regime between Josephson and Rabi (below the threshold coupling). Here we are fixing $N = 40$, $\mathcal{E}_J = 20$ and $k = 1$. The initial condition is $z \simeq 1$, $\phi = 0$.

Acknowledgements

APT and AF thank CNPq-Conselho Nacional de Desenvolvimento Científico e Tecnológico (a funding agency of the Brazilian Government) for financial support. JL gratefully acknowledges funding from the Australian Research Council and The University of Queensland through a Foundation Research Excellence Award. APT and AF would like to acknowledge GN Santos Filho for discussions.

References

- [1] E. A. Cornell and C. E. Wieman, *Rev. Mod. Phys.* **74** (2002) 875
- [2] J. R. Anglin and W. Ketterle, *Nature* **416** (2002) 211
- [3] E. A. Hinds and I. G. Hughes, *J. Phys. D: Appl. Phys.* **32** (1999) R119
- [4] R. Folman, P. Krueger, J. Schmiedmayer, J. Denschlag and C. Henkel, *Adv. Atom. Mol. Opt. Phys.* **48** (2002) 263
- [5] A. J. Leggett, *Rev. Mod. Phys.* **73** (2001) 307
- [6] M. H. Anderson, J. R. Ensher, M. R. Mathews, C. E. Wieman and E. A. Cornell, *Science* **269** (1995) 198
- [7] J. R. Anglin, P. Drummond, A. Smerzi, *Phys. Rev. A* **64** (2001) 063605

- [8] Y. Makhlin, G. Schön and A. Shnirman, *Rev. Mod. Phys.* **73** (2001) 357
- [9] L. Sanz, R. M. Angelo and K. Furuya, *J. Phys. A: Math. Gen.* **36** (2003) 9737
- [10] R. Botet, R. Jullien and P. Pfeuty, *Phys. Rev. Lett.* **49** (1982) 478
- [11] R. Botet and R. Jullien, *Phys. Rev. B* **28** (1983) 3955
- [12] H. J. Lipkin, N. Meshkov and A. J. Glick, *Nucl. Phys. B* **62** (1965) 188
- [13] A. J. Glick, H. J. Lipkin and N. Meshkov, *Nucl. Phys. B* **62** (1965) 211
- [14] H.-Q. Zhou, J. Links, R. M. McKenzie, X.-W. Guan, *J. Phys. A: Math. Gen.* **36** (2003) L113
- [15] J. Links, H.-Q. Zhou, R. M. McKenzie, M. D. Gould, *J. Phys. A: Math. Gen.* **36** (2003) R63
- [16] G. J. Milburn, J. Corney, E. M. Wright, D. F. Walls, *Phys. Rev. A* **55** (1997) 4318
- [17] Z.-D. Chen, J.-Q. Liang, S.-Q. Shen and W.-F. Xie, *Phys. Rev. A* **69** (2004) 023611
- [18] A. Smerzi and S. Raghavan, *Phys. Rev. A* **61** (2000) 063601
- [19] A. P. Tonel, J. Links and A. Foerster, *J. Phys. A: Math. Gen.* **38** (2005) 1235
- [20] A. P. Hines, R. H. McKenzie and G. J. Milburn, *Phys. Rev. A* **67** (2003) 013609
- [21] J. Vidal, G. Palacios and C. Astangul, *cond-mat/0406481*
- [22] F. Pan and J. P. Draayer, *cond-mat/0410423*
- [23] G. Kalosakas and A.R. Bishop, *Phys. Rev. A* **65** (2002) 043616
- [24] G. Kalosakas, A.R. Bishop and V.M. Kenkre, *Phys. Rev. A* **68** (2003) 023602
- [25] G. Kalosakas, A.R. Bishop and V.M. Kenkre, *J. Phys. B* **36** (2003) 3233
- [26] S. Kohler and F. Sols, *Phys. Rev. Lett.* **89** (2002) 060403
- [27] L. Bernstein, J. C. Eilbeck and A. C. Scott, *Nonlinearity* **3** (1990) 293
- [28] A. Micheli, D. Jaskch, J. I. Cirac, P. Zoller, *Phys. Rev. A* **67** (2003) 013607
- [29] T.-L. Ho, V. B. Shenoy, *Phys. Rev. Lett.* **77** (1996) 3276
- [30] S. Raghavan, A. Smerzi, S. Fantoni and S.R. Shenoy, *Phys. Rev. A* **59** (1999) 620
- [31] M. Albiez, R. Gati, J. Fölling, S. Hunsmann, M. Cristiani and M.K. Oberthaler, *Preprint cond-mat/0411757*